Research Article

Chemical Reaction Effects on Maxwell Base MHD Fluid Flow of Nonomaterial over Vertical Moving Surface with Radiation

KonduruVenkateswaraRaju[a*] Ravuri Mohana Ramana[b] MalrajuChangalRaju[c] KodiRaghunath[d]

[a*] Department of BS &H (Mathematics), ChadalawadaRamanamma Engineering College (Autonomous), Reniguntaroad,Tirupati-517506,Andhra Pradesh, India.
[b] Department of BS &H (Mathematics), Narasaraopeta Engineering College (Autonomous) Narasarapeta-522601 Andhra Pradesh, India.
[c] Dept. of Mathematics,JNTUA college of Engineering,Pulivendula,YSR Kadapa -516390, India.
[d]Assistant Professor, Department of Humanities and Sciences, Bheema Institute of Technology and Science, Adoni, Andhra Pradesh, Pin-518301, India.

Article History: Received: 11 January 2021; Revised: 12 February 2021; Accepted: 27 March 2021; Published online: 23 May 2021

Abstract: This research report investigated the laminar Maxwell Nanofluid boundary flow of MHD over a vertically moving flat porous plate in 2D (two dimensional). Consideration is given to viscous dissipation in conjunction with heat absorption. By employing appropriate similarity transformations, the governing PDEs are converted to a system of coupled nonlinear ODEs. Bvp4c solves the condensed equations using the firing technique. Graphs and tables illustrate the impacts of various parameters on velocity, temperature, and concentration profiles. We also evaluated the effect of multiple parameters on the skin friction coefficient, heat and mass transfer rate, and the Nusselt and Sherwood numbers, respectively.

Keywords: Healthy Maxwell fluid, Magneto hydrodynamics, Chemical reaction parameter, Radiation, Viscous dissipation.

1. Introduction:

Nowadays, non-Newtonian liquid flow analysis has gained popularity due to the numerous applications in research and technology. Researchers' insight into these fluids is due to their multiple uses, most notably in food goods, biological material, and chemical material. There are various industrial and natural applications for such fluids, such as molten polymers, paints, oils, drilling mud, polycrystal melts, fluid suspensions, cosmetic and food items, etc. All non-Newtonian fluids are prone to phenomena under shear that are not described by a single fundamental relationship.

Non-Newtonian liquids are recognized by individual models, for example, Maxwell (1867), Barus (1893), Jaffrey (1915), Sisko (1950), Bingham (1922), power law (1923), Williamson (1929),Eyring–Powell (1936), Generalized Burger(1939), Oldroyd-A (1950), Oldroyd-B (1950), Oldroyd-8 constant (1950), Casson (1959), Cross (1965),Carreau (1972), and Carreau–Yasuda (1972). Casson, Maxwell, and Williamson fluids each have relevance in the literature due to their unique properties. G. Narender et al. [2019] determined the convection of Maxwell Nanofluid across a stretching sheet with the effects of viscous indulgence and chemical reaction. Noor [2012] introduces the magnetohydrodynamics (MHD) stream of Maxwell fluid in thermophoresis and chemical reaction on a vertical sheet. Akbar et al. [2009] studied the thermal pollution, and MHD effect on a Maxwell fluid stretched across a sheet. Swati Mukhopadhyay et al. [2012] investigated the unsteady flow of a Maxwell fluid across an extended surface in the presence of a chemical reaction. S. Mukhopadhyay [2012] examined the effects of transpiration and internal heat generation/absorption on the unsteady flow of a Maxwell fluid at a stretched surface.

Radiation is a technique used to investigate the heat transfer of materials in a magnetic environment. In practically all industrial operations, radiative-convective fluxes occur. For example, heating and cooling chambers, energy processes involving fuel burning, and evaporation from huge open water reservoirs. The term radiative is critical in the field of heat and mass transfer studies.

Nanofluid is a term that refers to the interaction of nanoparticles with a fluid. Nanoparticles are frequently composed of carbides or carbon nanotubes, ethylene, glycol, and oil, which are all examples of based fluids. Nanofluids are primarily used in heat transmission. They demonstrate imposed thermal conductivity and convective heat transfer coefficients offset from those of the base fluid. Choi (1995) pioneered the concept of nanofluids, which are composed of evenly suspended and distributed nanometer-sized particles in a base fluid. Due to their increased thermal conductivity over the base fluid, these fluids are utilized to improve thermal conductivity and suspension stability in various industrial applications. Numerous studies on nanofluids (i.e., mixtures of fluid and nanoparticles) demonstrate that they can increase the thermal conductivity of fluids.

Studying the MHD flow of an electrically conducting fluid is critical in current metallurgical and metalworking operations. Metal melting, power generation, and nuclear reactor cooling are all examples of such fields. MHD flow may be used to extract polymer sheet from a die or to draw plastic films. Micropolar MHD flow across a stretched sheet offers various applications, including polymer blends, porous rocks, aerogels, alloys, and microemulsions. K. Jabeen et al. [2020] investigated the thermophoresis, radiation, and chemical reaction analyses of MHD fluids in porous media. P. Chandra Reddy et al. [2019] investigated the buoyancy effects on a chemically reactive magneto nanofluid passing through a moving vertical plate. K. Venkateswara

Raju et al. [2021] investigated the convective boundary flow and source of heat in an MHD Casson Fluid passing through a stretched sheet.

If an unexpected ingredient such as air or water is present, a chemical reaction is noticed. When two species interact chemically, heat is created. Generally, the rate of reaction is proportional to the species' concentration. If the reaction rate is directly proportional to the speed of relative fixation, it is said to be of the first order. Stanford Shateyi [2013] used a numerical approach to investigate the MHD flow of a Maxwell fluid past a vertical stretching sheet in the presence of thermophoresis and chemical reaction. Await al.[2015] investigated the effects of Maxwell Fluid flow over a Permeable Surface with Chemical Reaction: Dual Solutions on Maxwell Fluid flow. Mohana Ramana et al.[2020] investigated the effects of softening and radiation on the MHD heat and mass transfer of Casson fluid flowing past a porous extending sheet in the presence of a chemical reaction.

2. Mathematical formulation

The laminar, two-dimensional frontier layer flow of an incompressible nonNewtonian Maxwell fluid over an unstable extending sheet is considered in this section. The magnetic field that is begun is much weaker than the magnetic field that is administered. Thus, at low magnetic Reynolds numbers, the induced magnetic field is ignored.

The $x-$ axis is considered toward vertically moving flat plate where as $y-$axis is perpendicular to it. Both concentration and thermal buoyancy effects are of significant importance. Let C_w be the concentration at the sheet surface and the concentration far away from the sheet is C_∞. We have believed the fluid to be heat retaining with impacts of thermal radiation, chemical reaction and thick dissipation. The temperature at the surface is considered at T_w and T_∞ far away from the plate. We are given a free stream velocity $u = U_w(x)$, is given to the vertically moving surface. The 2D MHD frontier layer equations of an incompressible Maxwell nanofluid are

$$\frac{\partial u^*}{\partial x} + \frac{\partial v^*}{\partial y} = 0 \quad (1)$$

$$u^* \frac{\partial u^*}{\partial x} + v^* \frac{\partial v^*}{\partial y} + \lambda\left(u^{*2}\frac{\partial^2 u^*}{\partial x^2} + v^{*2}\frac{\partial^2 u^*}{\partial y^2} + 2u^* v^* \frac{\partial^2 u^*}{\partial y \partial x}\right) = -\frac{1}{\rho}\frac{\partial p^*}{\partial x} + \vartheta\left(\frac{\partial^2 u^*}{\partial y^2}\right) - \frac{\sigma {B_0}^2}{\rho}u^* + g_0\beta_T(T^* - T_\infty) + g_0\beta_c(\mathrm{C}^* - C^*{}_\infty) \quad (2)$$

$$u^* \frac{\partial T^*}{\partial x} + v^* \frac{\partial T^*}{\partial y} = \alpha\left(\frac{\partial^2 T^*}{\partial y^2}\right) + \frac{16\sigma^*}{3k^*}\frac{T_\infty}{(\rho C_p)_f}\frac{\partial^2 T^*}{\partial y^2} + \tau\left(D_B\frac{\partial C^*}{\partial y}\frac{\partial T^*}{\partial y} + \frac{D_T}{D_\infty}\left(\frac{\partial T^*}{\partial y}\right)^2\right) + \frac{\mu}{(\rho C_p)_f}\left(\frac{\partial u^*}{\partial y}\right)^2 - \frac{Q_0}{(\rho C_p)_f}(T^* - T^*{}_\infty) \quad (3)$$

$$u^* \frac{\partial C^*}{\partial x} + v^* \frac{\partial C^*}{\partial y} = D_B\frac{\partial^2 C^*}{\partial y^2} + \frac{D_T}{T_\infty}\frac{\partial^2 T^*}{\partial y^2} - K_r(C^* - C_\infty) \quad (4)$$

With respect to boundary conditions

$$u^* = U^*{}_w(x), v^* = V^*{}_w(x),\ T^* = T_w,\ C^* = C^*{}_w,\ \text{at y} = 0; \quad (5)$$

$$u^* \to U^*{}_w(x),\ T^* \to T_w,\ C^* \to C^*{}_w,\ \text{at y} \to \infty; \quad (6)$$

Where u and v are the parts of velocity respectively in the x and y ways., ϑ is the kinematic consistency of the fluid, C is the concentration of the species of the fluid, $U^*{}_w(x^*)$, is wall dimensional velocity and $V^*{}_w(x^*)$ is dimensional mass flux velocity with $V^*{}_w(x^*) > 0$ for infusion and $V^*{}_w(x^*) < 0$ for suction. $T_w{}^*, \mathrm{C}_w{}^*$ are wall dimensional temperature and concentration $U^*{}_e(x^*), T_\infty{}^*, \mathrm{C}_\infty{}^*$ are dimensional free stream velocity, temperature and concentration respectively. Outside the boundary layer, Eqs.(2) gives

$$-\frac{1}{\rho}\frac{dP}{dx}=\lambda U_e{}^2\frac{d^2U_e}{dx^2}+U_e\frac{dU_e}{dx}+\frac{\sigma B_0{}^2}{\rho}U_e \text{ (7)}$$

The dimensionless frontier layer variables are

$$x=\frac{x^*}{L};\ \mathrm{y}=\mathrm{R}_e{}^{1/2}\left(\frac{y^*}{L}\right);\ u=\left(\frac{u^*}{U_0}\right);\ v=\mathrm{R}_e{}^{1/2}\left(\frac{v^*}{U_0}\right);\ u_e(x)=\frac{U^*{}_e(x)}{U_0};\ K_1=\frac{K_r}{u_e x^{-2/3}}$$ (Chemical reaction parathion) $$u_w(x)=\frac{U^*{}_w(x)}{U_0};\quad v_w(x)=R_e{}^{1/2}\frac{V^*{}_w(x)}{U_0};\quad \theta=\frac{T^*-T^*{}_\infty}{T^*{}_w-T^*{}_\infty};\quad \phi=\frac{C^*-C^*{}_\infty}{C^*{}_w-C^*{}_\infty};$$

$$p=\frac{p^*-p_\infty}{\rho_f U^2{}_0};\ \text{Where}\ U_0\text{, is the characteristic velocity} \qquad (8)$$

By use Eqs .(6)and (7), we attain the following scheme of equations

$$\frac{\partial u}{\partial x}+\frac{\partial v}{\partial y}=0 \text{ (9)}$$

$$u\frac{\partial u}{\partial x}+v\frac{\partial u}{\partial y}+\frac{\lambda U_0}{L}\left(u^2\frac{\partial^2 u}{\partial x^2}+v^2\frac{\partial^2 u}{\partial y^2}+2uv\frac{\partial^2 u}{\partial y\partial x}\right)=\left(\frac{\lambda U_0}{L}\right)u^2{}_e\frac{d^2u_e}{dx^2}+u_e\frac{du_e}{dx}+\frac{\partial^2 u}{\partial y^2}$$
$$+\left(\frac{\sigma B_0{}^2 L}{\rho U_0}\right)(u_e-u)+\left(\frac{g_0\beta_T L}{U_0{}^2}\right)(T_w-T_\infty)\theta+\left(\frac{g_0\beta_c L}{U_0{}^2}\right)(\mathrm{C}_w-C_\infty)\phi \qquad (10)$$

$$u\frac{\partial\theta}{\partial x}+v\frac{\partial\theta}{\partial y}=\frac{1}{\mathrm{Pr}}\frac{\partial^2\theta}{\partial y^2}+\frac{U_0{}^2}{C_p(T_w-T_\infty)}\left(\frac{\partial u}{\partial y}\right)^2+\frac{4R}{3\mathrm{Pr}}\frac{\partial^2\theta}{\partial y^2}+N_b\frac{\partial\theta}{\partial y}\frac{\partial\phi}{\partial y}+N_t\left(\frac{\partial\theta}{\partial y}\right)^2$$
$$-\frac{Q_0 L}{(\rho C_p)_f U_0}\theta \qquad (11)$$

$$u\frac{\partial\phi}{\partial x}+v\frac{\partial\phi}{\partial y}=\frac{1}{\mathrm{Pr}}\left(\frac{1}{L_e}\frac{\partial^2\phi}{\partial y^2}+\frac{N_t}{N_b L_e}\frac{\partial^2\theta}{\partial y^2}\right)-K_1(C-C_\infty) \text{ (12)}$$

The dimensionless boundary conditions are defined by using equation (8) in equations (5&.6).

$$u=U_w(x), v=V_w(x),\ \theta=1,\ \phi=1,\ \text{as}\ \mathrm{y}=0; \text{ (13)}$$

$$u\to U_e(x),\ \theta\to 0,\ \phi\to 0,\ \text{as}\ \mathrm{y}\to\infty; \text{ (14)}$$

We assume that $u_w(x)$ and $u_e(x)$ have the following form $u_w(x)=u_w x^{1/3}$ and $u_e(x)=u_e x^{1/3}$ where u_w, u_e dimensionless constants are.

We introduce the similarity transformations here

$$\psi=U_e{}^{1/2}x^{2/3}f(\eta);\ \eta=U_e{}^{1/2}x^{-1/3}y;\ u=cxf'(\eta);\ v=-\sqrt{c\vartheta}f(\eta);$$

$$\eta=y\sqrt{\frac{c}{\vartheta}};\ \gamma=\frac{K_1}{c}\text{ (chemical reaction parameter) ;}$$

$$u=\frac{\partial\psi}{\partial y};\ \mathrm{v}=\frac{\partial\psi}{\partial x}(\text{stream functions}); \text{ (15)}$$

Thus we have $v_w(x)=-\frac{2}{3}U_e{}^{1/2}x^{-1/3}s$; where "$s$" , is non-dimensional transpiration parameter and $s>0, s<0$, represents suction and injection cases respectively.

After using the similarity transformations given in Eqs. (15),Eqs. (9) to (12) take the form

$$3(f'^2-1)-6ff''+2\beta(1-f'^3+\eta f'^2 f''+2f^2 f''')-9(f'''+M(1-f')+Gr\theta+Gc\phi)=0 \text{ (16)}$$

$$\frac{1}{\mathrm{Pr}}\left(1+\frac{4R}{3}\right)\theta''+Ecf''^2+N_b\theta'\phi'+N_t\theta'^2+\frac{2}{3}f\theta'-H\theta=0 \text{ (17)}$$

$$\phi'' + \frac{N_t}{N_b}\theta'' + \frac{2}{3}L_e P_r f\phi' - L_e \,\mathrm{PrK}_1\,\phi = 0 \quad (18)$$

Corresponding boundary conditions are

$$f(\eta) - s;\quad f'(\eta) - \gamma;\quad \theta(\eta) - 1;\quad \phi(\eta) - 1;\quad at\ \ \eta = 0; \quad (19)$$

$$f(\eta) - 1;\ \ \theta(\eta) - 0;\ \ \phi(\eta) - 0 \quad as \quad \eta \to \infty; \quad (20)$$

Where $\gamma = \frac{u_w}{u_e}$, is no-dimensional parameter for moving flat plate. If moving flat surface and free stream are parallel then $\gamma > 0$,but if anti-parallel then $\gamma < 0$ and $\gamma = 0$, for plate at rest. Te non-dimensional parameter are given below

$$\beta = \frac{\lambda U_0 U_e x^{-2/3}}{L}; \qquad M = \frac{\sigma {B_0}^2 L}{\rho U_0 U_e x^{-2/3}}; \qquad G_T = \frac{g_0 \beta_T L}{{U^2}_0 {U_e}^2 x^{-1/3}}(T_w - T_\infty) \quad ; \qquad K_1 = \frac{K_r}{\alpha};$$

$$G_c = \frac{g_0 \beta_c L}{{U^2}_0 {U_e}^2 x^{-1/3}}(\mathrm{C}_w - C_\infty); \qquad \mathrm{P} = \frac{\vartheta}{\alpha};\ R = \frac{4\sigma^* {T_\infty}^3}{k^* k_f}; \qquad Ec = \frac{{U^2}_0 {U_e}^2}{C_p - 2/3(T_w - T_\infty)};$$

$$N_b = \frac{\tau D_B}{\vartheta}(\mathrm{C}_w - C_\infty);\ \ N_t = \frac{\tau D_T}{\vartheta T_\infty}(T_w - T_\infty);\ \ \mathrm{H} = \frac{Q_0 L}{\left(\rho C_p\right)_f U_0 U_e x^{-2/3}};\ L_e = \frac{\alpha}{D_B}; \quad (21)$$

The final reduced equations (15)–(17) are evaluated numerically in mathematics software in conjunction with the corresponding boundary conditions given in Eqs. (19&20). With the similarity solution, the problem remains unchanged. First, we determine the symmetry group that converts one key of a differential equation to another explanation of the same differential equation. As a result, the solution is unchanged.

3. Nusselt number and Sherwood number

The Nusselt number Nu_x, is given as

$$Nu_x = \frac{x q_w}{k(T_w - T_\infty)}, \ \text{where}\ \ q_w = -k\left(1 + \frac{16\sigma^* {T_\infty}^3}{3k^* k_f}\right)\left(\frac{\partial T}{\partial y}\right)_{y=0} \quad (22)$$

And $\mathrm{Re}_x^{-1/2} Nu_x = -\left(1 + \frac{4R}{3}\right)\theta'(0),$

The Sherwood number is defined as

$$Sh_x = \frac{x h_m}{D_B(C_w - C_\infty)}, \ \text{where}\ \ \mathrm{h}_m = -D_B\left(\frac{\partial \phi}{\partial y}\right)_{y=0}; \quad (23)$$

$$\mathrm{Re}_x^{-1/2} Sh_x = -\phi'(0) \quad (24)$$

4. Results and Discussion

The nonlinear and linked systems Ordinary differential equations (16) - (18) are numerically solved using the Runge-Kutta method. Simultaneously, we investigated the effect of various physical factors on the flow field visually; we analyzed identical dimensionless variables on the friction factor, local Nusselt, and Sherwood numbers. In the graphs, $f'(\eta), \theta(\eta)$ and $\phi(\eta)$ signify the flow fields (velocity, temperature, and concentration respectively).In these calculations, we consider the entrenched variables for the graphical investigation as $R = 0.5,\ Nb = 1.0,\ M = 5,\ Ec = 0.1,\ Le = 0.5,\ \mathrm{K}_1 = 0.5,\ S = 0.5,\ Gt = 1.5,\ Gc = 1,$ $Nt = 0.9,\ e = 0.5$ while other parameters are varied over a range which is listed in figure captions.

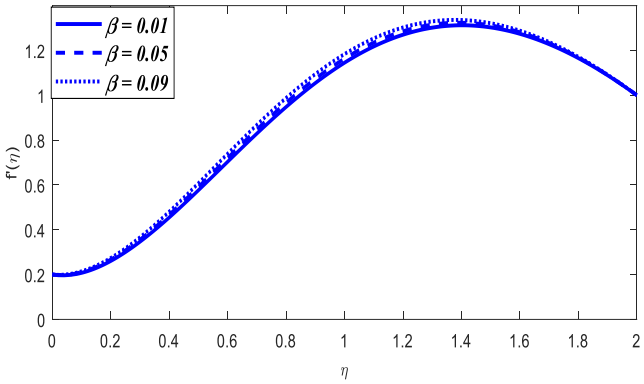

Figure.1: Velocity distribution for β ,

Where $g = 0.2$, $Le = K_1 = S = e = 0.5,\ Gt = 1.5,\ Gc = 1,\ Nt = 0.9,$

The resulting profiles of the dimensionless velocity $f'(\eta)$ distribution for various values of the Deborah number β , when $R = H = K_1 = 0.5, \mathrm{G}_c = 1, \mathrm{G}_t = 1.5,$ are displayed in Figure 1. It is observed that the velocity and boundary layer thickness are increasing functions of the Deborah number β . It should be pointed out that $\beta = 0$ represents Newtonian fluid and $\beta > 0$ represents the Jeffrey fluid parameter. The effect is found to increase the velocity distribution when β increased. Physically, viscous force produces a frictional force and it prevents the velocity of the fluid. By this reason, velocity is diminished for the augmented values of β .

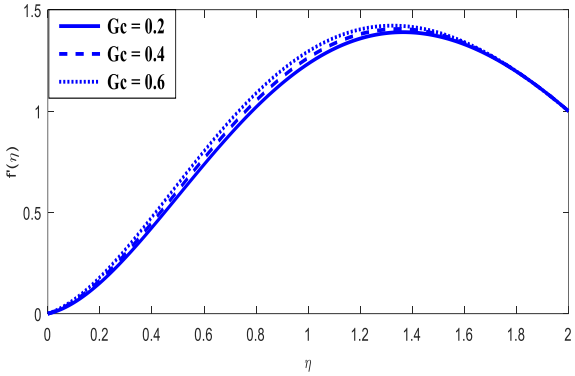

Figure.2: Velocity distribution for Gc

Where $g = 0$, $\beta = 0.1$ $Le = K_1 = S = e = 0.5,\ Gt = 1.5,\ Nt = 0.9,$

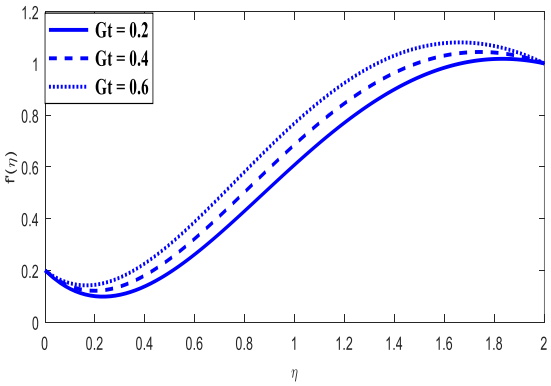

Figure.3: Velocity distribution for Gt

Where $g = 0$, $\beta = 0.1$ $Le = K_1 = S = e = 0.5,\ Nt = 0.9,$

The type of velocity under the influence of Gr and Gt is seen in Figures 2&3. Figures 2&3 illustrate the Grashof number of mass transfer and heat conduction on momentum. Again, the pattern is identical. The impact of the heat transfer's Grashof number on velocity increases the corresponding profile, as seen in Figures 2&3.

This is because the Grashof number is inversely proportional to the viscous force, and so as both numbers rise, the viscous force reduces, increasing the flow velocity.

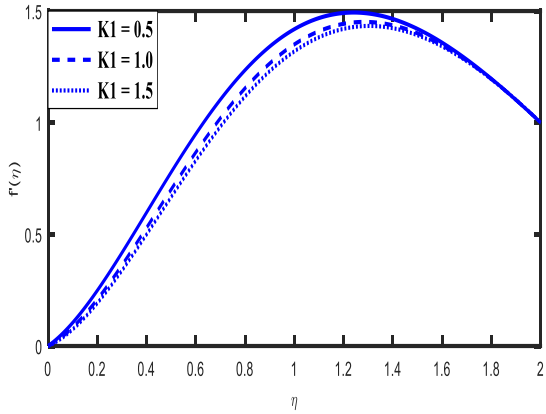

Figure.4: Velocity distribution for K_1

Where $g = 0$, $\beta = 0.1$ $Le = K_1 = S = e = 0.5,$ $Nt = 0.9,$

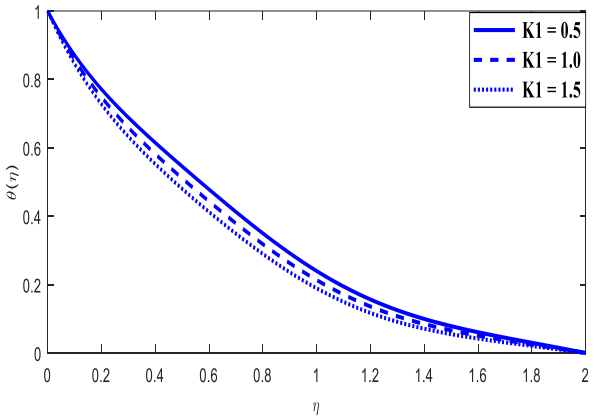

Figure.6: Temperature graphs for various values of K_1

The effect of the chemical reaction parameter on the velocity and temperature profiles of nanomaterials, respectively, Figure 4 and 6. It is discovered that increasing contributes to a reduction in the velocity and temperature distributions of nanomaterials. Chemical reactions have a lesser influence on the nanomaterial velocity than temperature profiles do

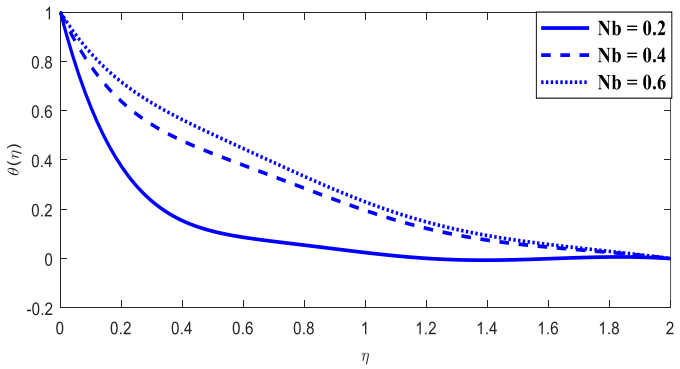

.

Figure.5: Temperature graphs for various values of N_b

As seen in Figure.5, raising the Brownian motion parameter results in a modest rise in the temperature profile and thickness of the boundary layer. Physically, different nanoparticles have an additional values of N_b . They are strengthening Brownian motion results in an increase in the fluid.

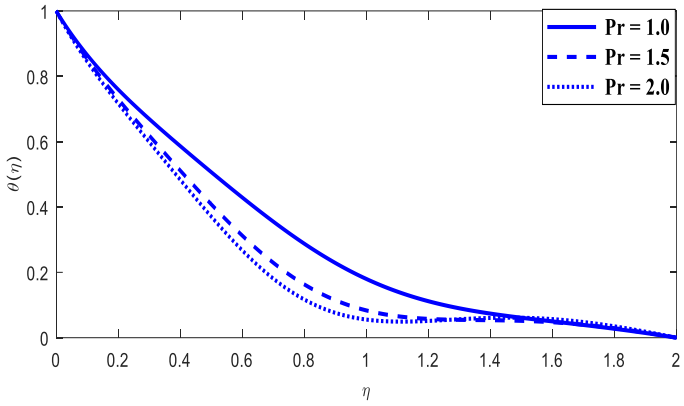

Figure.7: Temperature graphs for various values of $\Pr$

Figure 7 shows the impact of the Prandtl number on temperature $\theta(\eta)$ decrease with the increase of $\Pr$, this is due to the fact that a decrement is seen in the rate of heat transfer for enhancing values of $\Pr$.

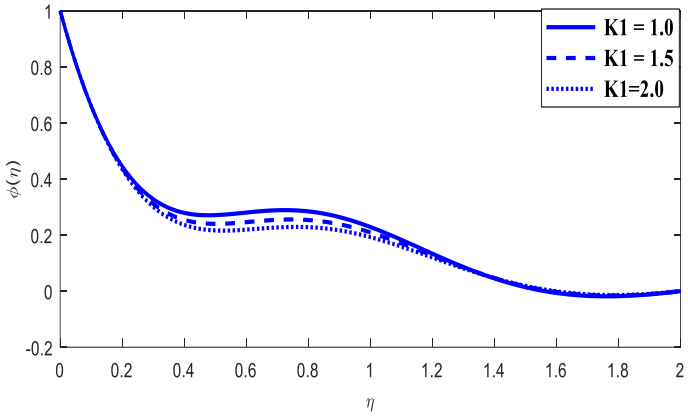

Figure.8: Concentration for distinct values of K_1

The chemical reaction parameter' K_1 effect on the concentration profile depicted in Figure 8. We note that the Concentration profile changes when the chemical reaction parameter K_1 is increased; in this case, we notice that the Concentration drops as it increases of K_1.

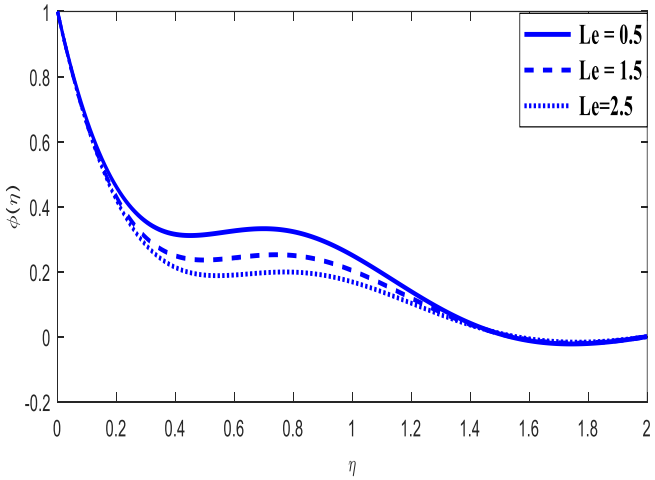

Figure.9: Concentration for distinct values of Le

The impact of Lewis number on concentration profiles is illustrated through Figure 9. The rate within thermal diffusivity and D_m is defined as Lewis number. From the figure, it can be observed that higher values of Lewis number decrease the concentration graph and the concentration boundary layer thickness. Thus, the mass diffusivity is reduced with the enlargement of Le, hence $\phi(\eta)$ is declined.

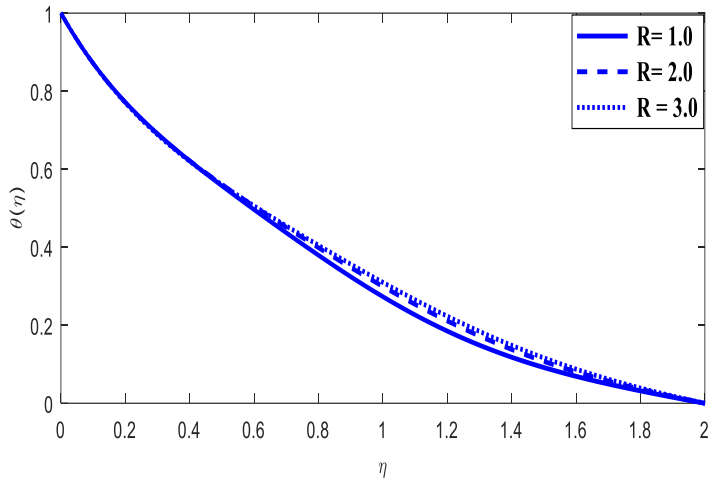

Figure.10: Temperature for distinct values of R

Figure.10 predicts the temperature profile for different values of the rotational parameter R. The results show that the temperature decreases with an increasing of R.

Table.1

M	K_1	Le	Nt	Nb	Sf	Nu	Sh
1					-1.771178	-5.189051	1.087005
2					-1.569176	-6.223102	1.254606
3					-1.452163	-7.023509	1.370314
	1				-1.179110	-8.002466	1.418070
	2				-1.184873	-8.006552	1.440850
	3				-1.188462	-8.006765	1.451034
		0.5			-1.175286	-7.998751	1.401132
		1			-1.996622	-8.049352	1.373259
		1.5			-1.214588	-8.-89870	1.352162
			0.5		-1.175286	-7.998751	1.401132
			1		-0.503753	-6.136503	2.306851
			1.5		-0.096352	-5.030203	2.832586
				0.5	-1.175286	-7.998751	1.401132
				1	-1.179524	-8.073220	0.822352
				1.5	-1.200462	-8.168087	0.635460

5. Conclusions

We developed a computational model to investigate the effect of Chemical Reactions and Radiation on Nanomaterial Maxwell Base MHD Fluid Flow. The Runge-Kutta and shot methods provide numerical answers for changing over ODEs to see the fluid flow visually. The following are critical repercussions of the present probe.

- The nanomaterial velocity and fluid temperature profiles are decreased for extending calculations of the chemical reaction parameter K_1.
- When the Lewis number is increased, the Distribution of Concentration decreases.
- Temperature profiles of the nanoparticles increase as the Radiation parameter is increased.

$x, y(m)$	Cartesian coordinate system	N_t	Thermo phoresis parameter
β	Deborah number	H	Heat absorption parameter
M	Hartmann number	L_e	Lewis number
$\vartheta(m^2 s^{-1})$	Kinematic number	Q_0	Heat absorption coefficient
G_t	Thermal grashoff parameter	$h_m(kg\ s^{-1}\ m^{-2})$	Surface mass flux
Pr	Prandtal number	N_b	Brownian motion parameter
R	Radiation parameter	G_c	Concentration grashoff parameter
D_B	Brownian diffusion coefficient	D_T	Thermophoretic diffusion coefficient
$q_w(W\ m^{-2})$	Surface heat flux	**Greek symbols**	
γ	Chemical reaction parameter	k^*	Mean absorption coefficient
E_c	Eckert number	σ^*	Stefan Boltzmann coefficient

6. References:

1. Akbar, V. A., Alizadeh-Pahlavan A., and Sadeghy, K. (2009).The influence of thermal radiation on MHD flow of Maxwell fluids above stretching sheets. Communications in Nonlinear Science and Numerical Simulation.Vol. 14, No.3, pp. 779-794.
2. Amit Parmar, and Shalini Jain.(2018). Radiative boundary-layer flow of an MHD Maxwell fluid with non-linear chemical reaction and heat source in a permeable channel, International Journal of Heat and Technology, Vol. 36, No. 4, pp. 1450-1455.
3. Awais, M., Muhammad, N., Hayat, T. and Alsaedi, A. (2015).Chemical Reaction Effects in Maxwell Fluid Flow Over Permeable Surface: Dual Solutions. IJNSNS, Vol.16, No.2, pp.: 123–128, https://doi.org/10.1515/ijnsns-2014-0093.
4. Chandra Reddy, P., Venkateswara Raju, K., Umamaheswar, M., and Raju , M. C. (2019). Buoyancy effects on chemically reactive Magneto- nanofluid past a moving vertical plate, Bulletin of pure and applied sciences,Vol.38, No.1,pp.193-207, www,bpasjournals.com
5. Jabeen, K., Mushtaq, M. and AkramMuntazir, R. M. (2020). Analysis of MHD fluids around a linearly Stretching Sheet in Porous Media with thermophoresis, radiation, and Chemical reaction,Hindawi Mathematical Problems in Engineering, pp.1-14, https://doi.org/10.1155/2020/9685482
6. Mohana Ramana, R., Girish Kumar, J, and Venkateswararaju K. (2020). Melting and radiation effects on MHD heat and mass transfer of Casson fluid flow past a permeable stretching sheet in the presence of chemical reaction, AIP CONFERENCE PROCEEDINGS, 2246, 020021; https://doi.org/10.1063/5.0014732
7. Mukhopadhyay, S. and Vajravelu, K. (2012). Effects of transpiration and internal heat generation/absorption on the unsteady flow of a Maxwell fluid at a stretching surface, ASME J. Appl. Mech.http://dx.doi.org/10.1115/1.4006260
8. Narender, G., Govardhan, K. and Sreedhar Sarma, G. (2019). Convection of Maxwell Nanofluid with the Effects of Viscous dissipation and Chemical reaction over a Stretching sheet, AIP CONFERENCE PROCEEDINGS, https://doi.org/10.1063/5.0014544
9. Noor, N. F. M. (2012). Analysis for MHD flow of a Maxwell fluid past a vertical stretching sheet in the presence of thermophoresis and chemical reaction. World Acad. Sci., Eng. Technol, Vol. 64, pp. 1019-1023.
10. Stanford Shateyi.(2013).A new numerical approach to MHD flow of a Maxwell fluid past a vertical stretching sheet in the presence of thermophoresis and chemical reaction.,

http://www.boundaryvalueproblems.com/content/2013/1/196n,Vol.196,Shateyi Boundary Value problems,

11. Swati Mukhopadhyay, KrishnenduBhattacharyya.(2012). Unsteady flow of a Maxwell fluid over a stretching surface in presence of chemical reaction, Journal of the Egyptian Mathematical Society , http://dx.doi.org/10.1016/j.joems.2012.08.019,No:20, pp.229-234.
12. Venkateswara Raju, K., Durga Prasad, P. , Raju M. C. , Sivaraj , R. (2021). MHD Casson Fluid Flow Pasta Stretching Sheet with Convective Boundary and Heat Source, LECTURE NOTES IN MECHANICAL ENGINEERING,pp.559-572, https://doi.org/10.1007/978-981-15-4308-1_44
13. Wubshet Ibrahim, and MekonnenNegera.(2020). MHD slip flow of upper-convected Maxwell nanofluid over a stretching sheet with chemical reaction, Journal of the Egyptian Mathematical Society, Vol. 28:No. 7, https://doi.org/10.1186/s42787-019-0057-2